# SERCA1 Truncated Proteins Unable to Pump Calcium Reduce the Endoplasmic Reticulum Calcium Concentration and Induce Apoptosis✪

**Mounia Chami,* Devrim Gozuacik,* David Lagorce,* Marisa Brini,‡ Pierre Falson,** Gérard Peaucellier,§ Paolo Pinton,¶ Hervé Lecoeur,‖ Marie-Lyse Gougeon,‖ Marc le Maire,** Rosario Rizzuto,¶ Christian Bréchot,* and Patrizia Paterlini-Bréchot***

*The French Institute of Health and Medical Research Institut National de la Santé et de la Recherche Médicale (INSERM/Pasteur U370)/Necker Faculty Institute of Medicine, 75015 Paris, France; ‡Department of Biochemistry and Center for the Study of Biomembranes of the National Research Council (CNR), University of Padova, 35121 Padova, Italy; §National Center Scientific Research, URA 2156, Arago Laboratory, F66651 Banyuls sur mer, France; ‖Pasteur Institute, Unit of Viral Oncology, SIDA Department of Retrovirus, 75015 Paris, France; ¶Department of Experimental and Diagnostic Medicine, Section of General Pathology, 44100 Ferrara, Italy; and **URA Centre National de Recherche Scientifique (CNRS) 2096, CEA Saclay, 91191 Gif sur Yvette, France



***Abstract.*** By pumping calcium from the cytosol to the ER, sarco/endoplasmic reticulum calcium ATPases (SERCAs) play a major role in the control of calcium signaling. We describe two SERCA1 splice variants (S1Ts) characterized by exon 4 and/or exon 11 splicing, encoding COOH terminally truncated proteins, having only one of the seven calcium-binding residues, and thus unable to pump calcium. As shown by semiquantitative RT-PCR, S1T transcripts are differentially expressed in several adult and fetal human tissues, but not in skeletal muscle and heart. S1T proteins expression was detected by Western blot in nontransfected cell lines. In transiently transfected cells, S1T homodimers were revealed by Western blot using mildly denaturing conditions. S1T proteins were shown, by confocal scanning microscopy, to colocalize with endogenous SERCA2b into the ER membrane. Using ER-targeted aequorin (erAEQ), we have found that S1T proteins reduce ER calcium and reverse elevation of ER calcium loading induced by SERCA1 and SERCA2b. Our results also show that SERCA1 variants increase ER calcium leakage and are consistent with the hypothesis of a cation channel formed by S1T homodimers. Finally, when overexpressed in liver-derived cells, S1T proteins significantly induce apoptosis. These data reveal a further mechanism modulating $Ca^{2+}$ accumulation into the ER of nonmuscle cells and highlight the relevance of S1T proteins to the control of apoptosis.

Key words: SERCA1 • endoplasmic reticulum • calcium • apoptosis • splice variants

## *Introduction*

Sarcoplasmic reticulum (SR)[1]/ER calcium ATPases (SERCAs) are calcium pumps that couple ATP hydrolysis with calcium transport across the SR/ER membrane (MacLennan et al., 1997). As a consequence of this activity, they maintain a level of resting intra-ER free calcium that is three to four orders of magnitude higher than the cytosolic $Ca^{2+}$ concentration. This level is crucial to a variety of ER-dependent cellular functions, including synthesis, folding and export of proteins, nucleocytoplasmic transport, stress response, and the modulation of IP3 (inositol 1,4,5-triphosphate) and SERCA expression (Meldolesi and Pozzan, 1998). On the cytosolic side, SERCA proteins control the frequency of IP3-induced intracellular $Ca^{2+}$ oscillations (Camacho and Lechleiter, 1993; Lechleiter et al., 1998), which in turn have the potential to regulate multiple cellular processes (Berridge et al., 1998), including gene expression (Dolmetsch et al., 1997).

SERCAs contain 10 transmembrane domains (M1–M10), with seven $Ca^{2+}$-binding residues localized in M4, M5, M6, and M8 and a large cytosolic domain. This do-

✪The online version of this article contains supplemental material.

M. Chami and D. Gozuacik contributed equally to this work.

Address correspondence to Patrizia Paterlini-Bréchot, Unité INSERM 370, Institut Necker/Pasteur, 156, rue de Vaugirard, 75730 Paris Cédex 15, France. Tel.: 33-1-40615644. Fax: 33-1-40615581. E-mail: paterlini@necker.fr

[1]*Abbreviations used in this paper:* aa, amino acid; $[Ca^{2+}]_c$, cytosolic free calcium concentration; $[Ca^{2+}]_{er}$, ER intraluminal free calcium concentration; erAEQ, ER-targeted recombinant aequorin; GFP, green fluorescent protein; IP3, inositol 1,4,5-triphosphate; NAO, nonyl acridine orange; S1T, SERCA1 splice variant; S1T−4, SERCA1 splice variant lacking exon 11 and 4; S1T+4, SERCA1 splice variant lacking exon 11; SERCA, SR/ER calcium ATPase; SR, sarcoplasmic reticulum; tBuBHQ, 2,5-di-(tert-butyl)-1,4-benzohydroquinone.

main is made of two parts, one inserted between M2 and M3, containing the actuator (A) domain involved in the transduction of conformational changes, and one between M4 and M5, which contains the nucleotide ATP-binding (N) domain and the phosphorylation (P) domain. Upon binding of two $Ca^{2+}$ by SERCA, Asp-351 undergoes ATP-dependent phosphorylation followed by a change in the enzyme conformation and the release of $Ca^{2+}$ into the ER lumen (MacLennan et al., 1997; Toyoshima et al., 2000).

SERCAs are encoded by three homologous genes: SERCA1, SERCA2, and SERCA3 (Wu et al., 1995). Transcripts from these genes undergo alternative splicing in a developmentally and tissue-specific manner, giving rise to isoforms that differ in their COOH-terminal region (MacLennan et al., 1997). SERCA1a (adult form) and 1b (fetal form) are mainly expressed in fast-twitch skeletal muscle (Zhang et al., 1995); and SERCA2a, in slow-twitch skeletal and cardiac muscle, whereas SERCA2b is widespread (Wuytack et al., 1992). SERCA3 is expressed in several nonmuscle tissues at variable levels and is always coexpressed with SERCA2b (Lytton et al., 1992). SERCA3 transcripts are also spliced, giving rise to three isoforms: SERCA3a, SERCA3b, and SERCA3c (Martin et al., 2000).

At present, the physiological significance of this heterogeneity amongst SERCA isoforms is unclear. However, recent data from the literature have pointed out their differing subcellular localizations (Lee et al., 1997) and the switch from one SERCA isoform to another under conditions that induce the same cell type to differentiate or, conversely, to proliferate (Launay et al., 1999). As an example, isoform switch from the nonmuscle SERCA2b to muscle SERCA2a was observed during differentiation of the myoblastic cell line $BC_3H1$ (De Smedt et al., 1991).

Recently, some evidence has emerged to show that SERCA may also have a direct impact on the processes of apoptosis, differentiation, and cell proliferation (Ma et al., 1999; Sakuntabhai et al., 1999; Chami et al., 2000). According to a recent report, SERCA2a overexpression may lead to apoptosis (Ma et al., 1999). SERCA2b has been shown to be a stress-inducible protein (Caspersen et al., 2000), and the stress response is tightly linked to the control of apoptosis (Jolly and Morimoto, 2000). SERCA2b expression has also been shown to be modulated by the antiapoptotic protein Bcl2 (Kuo et al., 1998). Mutations of the SERCA2 gene have been associated with Darier-White disease, a dominant inherited dermatosis with abnormal epidermal cell differentiation and adhesion (Sakuntabhai et al., 1999). Furthermore, the implication of a SERCA gene in cell transformation has recently been suggested by the report of a SERCA1 gene clonal mutation, due to integration of the Hepatitis B virus genome, occurring in a human hepatocellular carcinoma but not in the corresponding nontumorous tissue. Viral integration was shown to cis-activate SERCA1 chimeric transcripts with the splicing of exon 4 and/or exon 11 (Chami et al., 2000).

To investigate whether exon 4 and/or exon 11 spliced SERCA1 transcripts are also expressed in normal liver, we have cloned all SERCA1 transcripts from this tissue. We show here that exon 4 and/or exon 11 spliced SERCA1 splice variants (S1Ts) are expressed in liver as well as in several other human adult and fetal tissues. S1T proteins are expressed and detectable, by Western blot, in non-transfected cell lines derived from human transformed and primary cells. The splicing of exon 11 creates a frameshift and a premature stop codon in exon 12. The encoded proteins lack the main part of cytosolic domains N and P and transmembrane segments M5 to M10, which include six of the seven $Ca^{2+}$-binding residues, thus avoiding calcium pumping. The overexpression of S1T proteins induces apoptosis in three different cell lines. It also reduces the steady state $Ca^{2+}$ level in the ER and increases ER $Ca^{2+}$ leakage. In cotransfection experiments, S1T proteins consistently reduce the higher steady state $Ca^{2+}$ level in the ER due to SERCA1 or SERCA2b overexpression.

These results provide evidence for a new mechanism modulating SERCA-dependent $Ca^{2+}$ accumulation into the ER, and for implication of S1T proteins in the control of apoptosis.

## Materials and Methods

### cDNA Cloning of S1T

Total RNA was extracted from normal liver using TRIzol (Life Technologies, GIBCO BRL) and quantified by optical density and agarose gel electrophoresis. 3 μg of liver-derived RNA was denatured with 10 U of RNasin (RNA guard, Pharmacia Biotech) and 10 pmol of SERCA1 exon 23 antisense primer (5′-gcgtctagacacagctctgcctgaagatgtgtcact-3′) in a 10-μl volume at 65°C for 5 min. Reverse transcription was performed in a 25-μl final volume after the addition of 1× buffer supplied with the enzyme, 0.4 mM of each deoxynucleotide and 20 U of Moloney murine leukemia virus reverse transcriptase (Life Technologies) at 42°C for 30 min. Amplification was performed on one-third of the cDNA by using exon 1 sense (5′-gcgctcgagatggaggccgctcatgctaaaacac-3′) and exon 23 antisense primers in a final volume of 50 μl containing 25 mM Tris-Cl (pH 8.9), 40 mM potassium acetate, 4% glycerol, 200 μM each of dNTP, 1 U Taq polymerase (Life Technologies), and 0.04 U of Vent exo$^+$ polymerase (New England Biolabs, Inc.) in a thermal cycler 480 (PerkinElmer). A hot start technique was used by adding magnesium chloride after the temperature reached 80°C. The touchdown PCR protocol was applied with denaturation at 94°C for 30 s, extention step at 70°C for 3 min, annealing temperature starting at 65°C for 30 s, and decreasing by 1°C every two cycles to 55°C, at which temperature 19 cycles were performed followed by the final step at 72°C for 10 min. Overall, 40 cycles were carried out. Amplified product was purified using the Qiaquick spin PCR purification kit (QIAGEN) and cloned into pcDNA3 vector (Invitrogen). Clones were screened by filter hybridization with the total SERCA1 probe. Positive clones were picked up in duplicate and screened using SERCA1 exon 4 and exon 11 specific probes. SERCA1 positive clones characterized by the splicing of exon 4 and/or of exon 11 [SERCA1 splice variant lacking exon 11 and 4 (S1T−4), and SERCA1 splice variant lacking exon 11 (S1T+4)] were then sequenced.

### Amplification of S1T Variants

PCR was performed on normalized cDNAs from different human adult and fetal tissues (MTC panels human I K1420-1 and human fetal K1425-1; CLONTECH Laboratories, Inc.). These cDNAs were generated from poly A$^+$ RNA and normalized to the mRNA expression of six different housekeeping genes (including glyceraldehyde-3-phosphate dehydrogenase and delta lactoferrin) to ensure an accurate assessment of the specificity and relative abundance of target mRNA. The human MTC panels as a whole are also normalized against one another, so that the results obtained using human I and human fetal panels could be compared. Hot start touchdown amplification was then performed as described above, but with the extension step at 70°C for 1 min. We used primers on SERCA1 exon 10 (sense primer: 5′-tatcattgacaaggtggatggggacat-3′) and exon 13 (antisense primer: 5′-cttgacaaacatcttgttgcccacagca-3′). These primers amplify SERCA1 cDNAs with and without exon 11 splicing.

### Generation of a Polyclonal Antibody Specific to S1T Proteins

A peptide corresponding to the 10 COOH-terminal amino acids (aa) of S1T proteins (RQHSPPWWRR) was synthetized (Sigma-Aldrich), conju-

gated to Keyhole limpet hemocyanin and injected i.v. with Freund's adjuvant in two New Zealand rabbits. Three immunizations were performed, and sera were collected at different times and purified by affinity chromatography against the peptide.

## Cell Lines

We used HuH7 cells, derived from human hepatocellular carcinoma, CCL13 cells (American Type Culture Collection) derived from liver tumor cells, HeLa cells (CCL-2; American Type Culture Collection) derived from human cervix epithelioid carcinoma, T-47D cells (HTB 133; American Type Culture Collection) derived from human infiltrating breast ductal carcinoma, LNCaP cells (CRL 1740; American Type Culture Collection) derived from human metastatic prostatic adenocarcinoma, and Hs27 (CRL 1634; American Type Culture Collection) derived from human newborn foreskin primary fibroblasts.

## Isolation of Microsomal Fraction and Immunoblotting

Liver microsomes were isolated as described (Maruyama and MacLennan, 1988). Proteins were treated with concentrated urea (20 mg/50 μg protein), 1.8% SDS, and 9% β-mercaptoethanol and heated at 100°C for 1 min. After SDS-PAGE (10%), proteins were electrotransferred onto PVDF membranes Immobilon™-P (Millipore). For immunodetection, we used guinea pig polyclonal antibody 79B (diluted 1:5,000) raised against rabbit fast-twitch skeletal muscle SERCA1 (gift from A. M. Lompré, The French Institute of Health and Medical Research, INSERM, Chatenay-Malabry, Ferance) and anti-S1T (diluted 1:1,000) according to a reported protocol (Fuentes et al., 2000). After 1 h contact with the secondary antibody, the signal was revealed with the SuperSignal West Pico solution chemiluminescent substrate (Pierce Chemical Co.). Dimers or aggregates were sought by 7% SDS-PAGE in heated samples without urea (Soulié et al., 1996). For the antibody neutralization test, after hybridization with the 79B antibody, we applied the Restore™ Western Blot Stripping buffer (Pierce Chemical Co.) for 10 min at room temperature. Next, we performed three washes for 10 min at room temperature with the TBS-Tween solution (10 mM Tris HCl, pH 7.5, 100 mM NaCl, 0.2% Tween 20 [Sigma-Aldrich]) and left the membrane overnight in the TBS-Tween–milk (5% milk). The next day, we mixed 20 μg of 79B antibody and 200 μg the SR antigen (sarco-endoplasmic reticulum from rabbit) in a TBS–milk solution and allowed it to be in contact overnight on a wheel device. This 1 ml mix was then added to 9 ml of TBS-Tween–milk solution and was used to hybridize the membrane for 1 h at room temperature.

## Cloning and Transient Transfection Analyses

S1T+4, S1T−4, and SERCA1 were cloned into pcDNA3.1 (Invitrogen), subcloned into the green fluorescent protein (GFP) fusion construct pEGFP-N1 (CLONTECH Laboratories, Inc.) vector and pcDNA3.1/Myc-His (Invitrogen) and used to transiently transfect cell lines (HuH7, CCL13, HepG2, COS7, and HeLa cells) using ExGen solution (Euromedex). We used pig SERCA2b cDNA cloned in PsG5 vector (Stratagene) (Brini et al., 2000). The expression of all our constructs was driven by the CMV promoter, except the pig SERCA2b cDNA (SV-40 promoter). For transient transfection, $3 \times 10^5$ cells were seeded in six-well plates. The next day, transfection was carried out with 0.2 μg pEGFP-N1 (GFP empty vector to test the transfection efficiency) and 1.8 μg of the construct of interest by using the ExGen product and the supplied protocol. Experiments for immunolabeling and with ER-targeted recombinant aequorin (erAEQ) cotransfection were performed on 13-mm glass coverslips. For aequorin measurements, we cotransfected 0.5 μg erAEQ plus 1.5 μg of the construct of interest (or 0.7 μg of each in the case of two constructs). Cells were washed three times in PBS buffer 20 h after transfection and analyzed 48 or 72 h after transfection.

## Immunohistochemistry

Transfected HuH7 cells were fixed in 4% paraformaldehyde and permeabilized with 0.2% Triton X-100 for 10 min. Anti-S1T antibody, diluted 1:25, was first saturated with $4.8 \times 10^6$ nontransfected HuH7 cells in 0.05% Tween and 1% BSA in 300 μl final volume for 2 h at 4°C. After centrifugation at 5,000 rpm for 5 min, the supernatant was collected. Nonspecific binding sites were blocked with 3% BSA for 1 h. Anti-S1T antibody was then used at 1:50 dilution in 3% BSA. Immunodetection was carried out using the Envision Plus system (Dako).

## Immunofluorescence and Confocal Microscopy Analysis

Transfected cells were fixed in 4% paraformaldehyde and permeabilized at 4°C for 10 min in cold methanol (−20°C). Nonspecific binding sites were blocked with 3% BSA. Immunostaining was performed with anti-SERCA2 monoclonal antibody (clone IID8; Novocastra Ltd.), diluted 1:200, or anti-mitochondria polyclonal antibody (gift from C. Marsac, Neckler Faculty of Medicine, Paris, France), diluted 1:200. Immunodetection was carried out using Cyanin5-conjugated secondary antibody diluted 1:200. Coverslips were analyzed using confocal laser scanning microscopy (LSM 510; ZEISS).

## Apoptosis

Apoptosis was assessed using two complementary approaches. Cells were analyzed 72 h after transfection with GFP fusion constructs. The percentage of apoptotic nuclei was counted in ≥600 transfected GFP-positive cells in at least three independent experiments using DNA-dye 7-amino actinomycin D (Sigma-Aldrich) nuclear staining. In parallel, a FACScan® flow cytometer was used to record the combination of alterations to the mitochondrial structure, assessed by nonyl acridine orange (NAO) incorporation (Petit et al., 1995) and cell size (Forward Scatter: FSC). After transfection with the pcDNA3 clones, adherent and floating cells were incubated for 30 min at 37°C in PBS containing 4 μM NAO before analysis. Data from $2 \times 10^4$ events were recorded on a logarithmic scale and analyzed using CellQuest software.

## Aequorin Measurements

The aequorin chimera targeted to the ER (erAEQ) (Montero et al., 1995) was transfected alone (control) or cotransfected with SERCA1, SERCA2b and/or S1T constructs in HuH7, CCL13, or HeLa cells. Aequorin measurements were performed as described (Pinton et al., 2000), 48 h after transfection in HeLa cells and 48 and 72 h after transfection in HuH7 and CCL13 cells. To achieve high efficiency reconstitution of the erAEQ, luminal ER free calcium concentration ($[Ca^{2+}]_{er}$) must first be reduced. This was obtained by incubating the cells for 1 h at 4°C in Krebs-Ringer modified buffer (KRB; 125 mM NaCl, 5 mM KCl, 1 mM $Na_3PO_4$, 1 mM $MgSO_4$, 5.5 mM glucose, and 20 mM Hepes, pH 7.4, at 37°C) supplemented with 5 μM n-coelenterazine, 5 μM of the $Ca^{2+}$ ionophore ionomycin, and 600 μM EGTA. After incubation, the cells were extensively washed with KRB supplemented with 2% BSA and 1 mM EGTA and then with 100 μM EGTA for 30 s. The coverslips were then transferred to the luminometer and perfused in KRB supplemented with 1 mM $CaCl_2$ solution until the plateau level was reached (refilling phase). To obtain lower $[Ca^{2+}]_{er}$ values in control cells, cells were perfused with KRB supplemented with 600, 300, or 100 μM $CaCl_2$ solution.

To analyze the $Ca^{2+}$ leak rate from the ER, after reaching the plateau level, $Ca^{2+}$ release was initiated by treating the cells with 50 μM 2,5-di-(tert-butyl)-1,4-benzohydroquinone (tBuBHQ) (SERCA pump inhibitor). The maximum rates of $Ca^{2+}$ release (measured from the first derivative) at different $[Ca^{2+}]_{er}$ values were calculated and plotted for S1T-transfected and control cells.

All aequorin measurements were carried out in KRB and terminated by lysing the cells with 100 μM digitonin in a hypotonic $Ca^{2+}$-rich solution (10 mM $CaCl_2$ in $H_2O$), thus discharging the remaining aequorin pool. The light signal was collected and calibrated into $[Ca^{2+}]$ values as previously described (Brini et al., 1995; Rizzuto et al., 1995). In brief, a 13-mm round coverslip with the transfected cells was placed in a perfused thermostated chamber located in close proximity to a low-noise photomultiplier, with built-in amplifier discriminator. The output of the discriminator was captured by a Thorn-EMI photon counting board and stored in an IBM-compatible computer for further analyses. Aequorin luminescence data were calibrated off-line into $[Ca^{2+}]$ values using a computer algorithm based on the $Ca^{2+}$ response curve of mutated-type aequorin, as previously described (Montero et al., 1995).

## Statistical Methods

Continuous variables were compared using Student's *t* test or a nonparametric (Mann-Whitney) test when their distribution was skewed. Categorical variables were compared using the Chi square test with Yates correction.

## Online Supplementary Material

Online supplementary Tables SI and SII show comparative analysis of $Ca^{2+}$ leak in HeLa (Table SI) and HuH7 (Table SII) cells transfected with

S1T constructs (S1T+4 and S1T−4) and in the corresponding nontransfected cells (NTC). Comparison of $Ca^{2+}$ leak values were only made between experiments having comparable levels of $[Ca^{2+}]_{er}$ (not exceeding 50 μM). This analysis revealed that the leak value is higher in S1T+4- and S1T−4-transfected cells than in nontransfected cells.

Online supplementary Figure A shows curves corresponding to selected leak values in Table SII (see codes under curves and in Table SII). These curves show also that the passive leak obtained after addition of tBuBHQ is higher in S1T+4- and S1T−4-transfected cells than in nontransfected cells (control).

Online supplementary Figure B shows the indication of the time interval needed to obtain a decrease of $[Ca^{2+}]_{er}$ from 120 to 57 μM in the profiles depicted in C of Fig. 7. This time interval is 165 s in nontransfected cells (control) and 28 and 37 s in S1T+4- and S1T−4-transfected cells, respectively. Supplementary material is available at http://www.jcb.org/cgi/content/full/153/6/1301/DC1.

## Results

### Cloning of Spliced SERCA1 Variants

We cloned SERCA1 transcripts from normal liver and obtained 25 clones. Upon analysis with full-length SERCA1, SERCA1 exon 11, and SERCA1 exon 4 specific probes, 17 clones corresponded to SERCA1 and 8 clones were found to be characterized by exon 11 splicing (S1T+4), including two that also exhibited exon 4 splicing (S1T−4). This result was confirmed by sequence analysis. Exon 11 splicing leads to a frameshift encoding 22 aa (PKVSMRRSARPPRQHSPPWWRR) followed by a premature stop codon in exon 12 (Fig. 1 A).

### Predicted Structure of S1T Proteins

According to the recently reported crystal structure of rabbit SERCA1a resolved at 2.6 Å (Toyoshima et al., 2000), the calcium-transporting ATPase (Fig. 1 B, left) is provided with two calcium-binding sites formed by the side-chain oxygen atoms of seven transmembrane residues and by the backbone oxygen atoms of three transmembrane residues (Toyoshima et al., 2000; Zhang et al., 2000). Calcium-binding site I is formed by side-chain oxygen atoms of Asn-768 (M5), Glu-771 (M5), Thr-799 (M6), Glu-908 (M8) (Fig. 1 B, ●) and of Asp-800 (M6), which also participates in calcium-binding site II (Fig. 1 B, ▲). Calcium-binding site II is formed by side-chain oxygen atoms of Asn-796 (M6), Glu-309 (M4) (◆), and Asp-800, and by the backbone oxygen atoms of Val-304 (M4), Ala-305 (M4), and Ile-307 (M4) (◇). In addition to that, calcium-binding is also controlled by L6/7 cytoplasmic loop in which three residues, Asp-813, Asp-815, and Asp-818 (■), play a critical role (Falson et al., 1997; Menguy et al., 1998).

The structural consequence of splicing of exon 11 in S1T+4 and S1T−4 is the deletion of transmembrane segments M5 to M10 (Fig. 1 B, middle and right). Thus, S1T proteins keep four of the six calcium-binding residues of calcium-binding site II, including Val-304, Ala-305, and Ile-307. These three residues participate in calcium binding by their backbone oxygen atom depending on their position in the whole protein three-dimensional structure, thus in S1T proteins their contribution to calcium binding could be compromised. In contrast, the fourth residue, Glu-309, is still able to interact with calcium by its side-chain oxygen atom. Moreover, in the new structural conformation of S1T, acidic or polar residues, in particular Glu-58 (M1), and probably also Gln-108 (M2), at least in

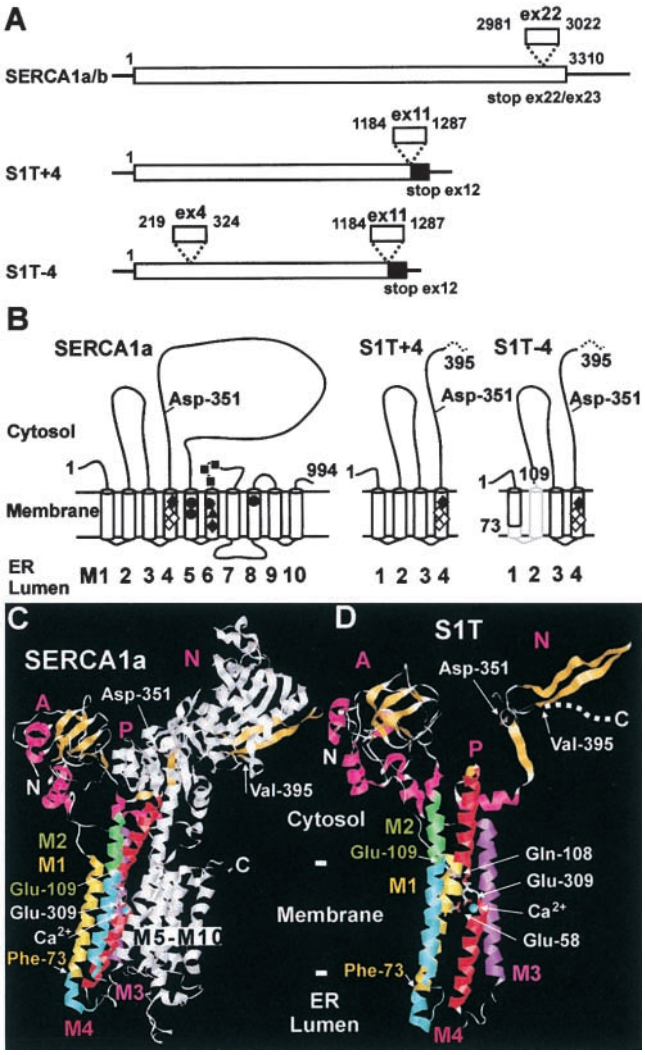


*Figure 1.* SERCA1 cDNA clones isolated from normal liver and the predicted structure of encoded proteins. (A) cDNA structure of the SERCA1 adult isoform with a stop codon in exon 22 (SERCA1a) and of the neonatal isoform characterized by exon 22 splicing and a stop codon in exon 23 (SERCA1b). Spliced isoforms (S1T+4 and S1T−4) are characterized by exon 4 and/or exon 11 splicing. Exon 11 splicing leads to a frameshift, encoding a 22-aa peptide (■), and a premature stop codon in exon 12. (B) Predicted topological structure of S1T proteins as compared with SERCA1. (Left) SERCA1. Numbers below drawings indicate transmembrane domains (M). Phosphorylatable Asp-351 is indicated. ● and ◆ indicate transmembrane residues involved in calcium-binding sites I and II, respectively, and that bind calcium by a side-chain oxygen atom. ▲ corresponds to the Asp-800 residue that participates in both sites I and II. ◇ correspond to residues involved in calcium-binding site II and that bind calcium by the backbone oxygen atom. ■ indicate cytoplasmic calcium-binding residues. (Middle and right) S1T proteins. The 22-aa COOH-terminal peptide is depicted as a dotted line, and the peptide (35 aa) encoded by exon 4 and deleted in S1T−4 is in gray (right). (C) Three-dimensional structure of rabbit SERCA1a, according to Toyoshima et al. (2000), using Rasmol 2.7.1 and the 1EUL PDB file (http://www.rcsb.org/pdb/cgi/explore.cgi?pdbId=1EUL, see supplementary materials for directions on viewing under different orientations). The A transduction (A), phosphorylation (P), and nucleotide-binding (N) domains are indicated. Secondary structures are displayed in ribbons. Those that are common to SERCA1 and S1T proteins are in color: β-sheets are in dark yel-

S1T+4, could help to create a new calcium-binding site (Fig. 1 D). Domains P and N are nearly completely removed in S1T proteins (Fig. 1, C and D), suggesting that they are neither able to bind ATP nor to transfer a phosphate on Asp-351, the residue that is reversibly phosphorylated during calcium transport. The frameshift created by splicing of exon 11 gives rise to 22 COOH-terminal mutated residues, depicted as an hypothetical structure (dotted line) in Fig. 1, B and D.

S1T−4 also lacks a peptide (74-VLAWFEEGEETITAFVEPFVILLILIANAIVGVWQ-108), depicted in blue in Fig. 1, C and D, corresponding to the last five COOH-terminal residues of M1, the connecting loop L1/2, and the main part of M2. As a consequence, residues Phe-73 and Glu-109 come in close contact (Fig. 1 B, right, C and D). This deletion is expected to deeply modify the remaining membrane domain of the protein. Its three-dimensional structure is, at present, unpredictable.

Therefore, according to their predicted structure and by analogy with previously reported SERCA1 mutants (MacLennan et al., 1998), S1T+4 and S1T−4 proteins, which expected size is 46 and 43 kD, respectively, cannot function as calcium pumps.

### *Spliced SERCA1 Variants Are Expressed in Human Adult and Fetal Tissues*

RT-PCR analysis of SERCA1 spliced transcripts was performed on different human adult and fetal tissues. We used a set of primers (see Materials and Methods) that coamplify SERCA1 cDNAs with or without exon 11 splicing (Fig. 2; SERCA1 and S1T). S1T are expressed in different human adult (pancreas, liver, kidney, lung, and placenta) and fetal (kidney, liver, brain, and thymus) tissues and are not expressed in adult skeletal muscle, heart, and brain and fetal skeletal muscle and heart (Fig. 2). The relative amount of S1T as compared with SERCA1 differed according to the tissue analyzed, and was higher in fetal liver, kidney, and brain than in the corresponding adult tissues. Although adult brain only expressed SERCA1, only S1T transcripts were detectable in the corresponding fetal tissue. These observations are consistent with a switch of

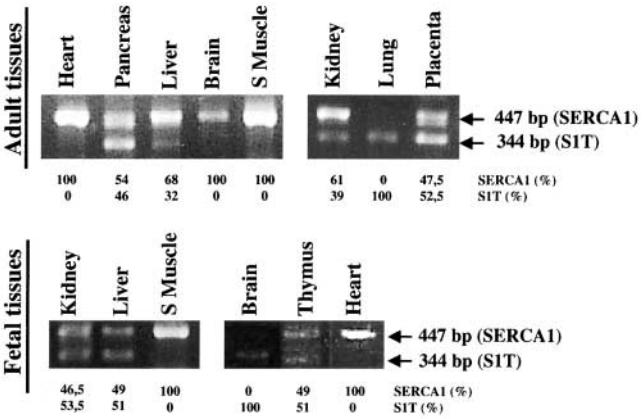


*Figure 2.* Amplification of native S1T transcripts of human adult and fetal tissues. Semiquantitative PCR analysis of S1T tissue expression patterns was performed with Marathon-ready cDNA (CLONTECH Laboratories, Inc.) using primers on SERCA1 exons 10 and 13. This set of primers amplifies SERCA1 transcripts with (447 bp; SERCA1) and without (344 bp; S1T) exon 11 splicing. S1T corresponds to the exon 11–spliced isoforms with or without exon 4 splicing (S1T+4 and S1T−4). Semiquantification was performed using the NIH image v1.62 program. Numbers below each lane indicate the proportion (%) of SERCA1 and S1T transcripts in each tissue.

SERCA1 to S1T expression in fetal cells. Our assessment is reliable for the following reasons: (a) RT-PCR results were reproducibly obtained on cDNAs normalized using the expression of several housekeeping genes (see Materials and Methods); (b) the relative amount of SERCA1 and S1T was estimated by using the same primer set which amplifies both cDNAs; and (c) the PCR product was obtained at the exponential PCR phase and semiquantified by image analysis (NIH program).

Thus, the variable expression pattern of S1T variants that we observed rules out their illegitimate transcription (Chelly et al., 1989) and is consistent with a biological function of the corresponding proteins.

### *S1T Proteins Are Expressed in Different Human-derived Cell Lines and Localize to the ER Membrane*

We used a polyclonal antibody (anti-S1T) selectively directed to the COOH-terminal 10 aa created by exon 11 splicing. Western blot analysis of microsomal fraction from cells transiently transfected with SERCA1 and S1T+4 allowed us to detect both SERCA1 and S1T+4 proteins using the 79B antibody, directed to the first cytoplasmic loop of SERCA1, and only the S1T+4 band using the anti-S1T antibody. S1T+4 was detected as a monomer (46 kD) in denaturing conditions (heated sample treated with urea) (Soulié et al., 1996) (Fig. 3 A). In the microsomal cellular fraction obtained from nontransfected CCL13, T-47D, and Hs27 cell lines, we found a clear 46-kD band using the anti-S1T antibody (Fig. 3 B) corresponding to the S1T+4 isoform. In fact, cloning analyses had shown that expression of the S1T−4 isoform is lower than that of the S1T+4 isoform. No bands were observed in microsomal samples from HeLa and LNCaP cell lines. The specificity of this finding was assessed by the neutralization assay shown in Fig. 3 C. By using the anti-SERCA 1 antibody 79B, we re-

low, and cytosolic α helices are in magenta. Residues from Leu-396 to Gly-994 (COOH-terminal) removed by the splicing of exon 11 in S1T are in gray. Transmembrane α helices M1, M2, M3, and M4 are depicted in yellow, green, violet, and red, respectively. The peptide Val-74 to Gln-108 encoded by exon 4 and deleted in the S1T−4 protein is indicated in blue. Residues Phe-73 and Glu-109, which come in contact in S1T−4, are indicated. Phosphorylatable Asp-351 and calcium-binding residue Glu-309 are also shown. Calcium ions are space filled and colored in cyan. (D) Hypothetical three-dimensional structure of S1T deduced from that of rabbit SERCA1a. Residue Val-395 in S1T is followed by a 22-aa COOH-terminal peptide generated by the frameshift and depicted as a dotted line. Its structure is unknown. The region colored in blue is removed in the S1T−4 protein and presumably leads to an important structural rearrangement. The position of the calcium atom located near residue Glu-309 is hypothetical. Residues Glu-58 and Gln-108, which are close to Glu-309 and may participate in the channelling of calcium in S1T+4 dimers along the side of transmembrane domains M2–M4, are displayed in wireframe.

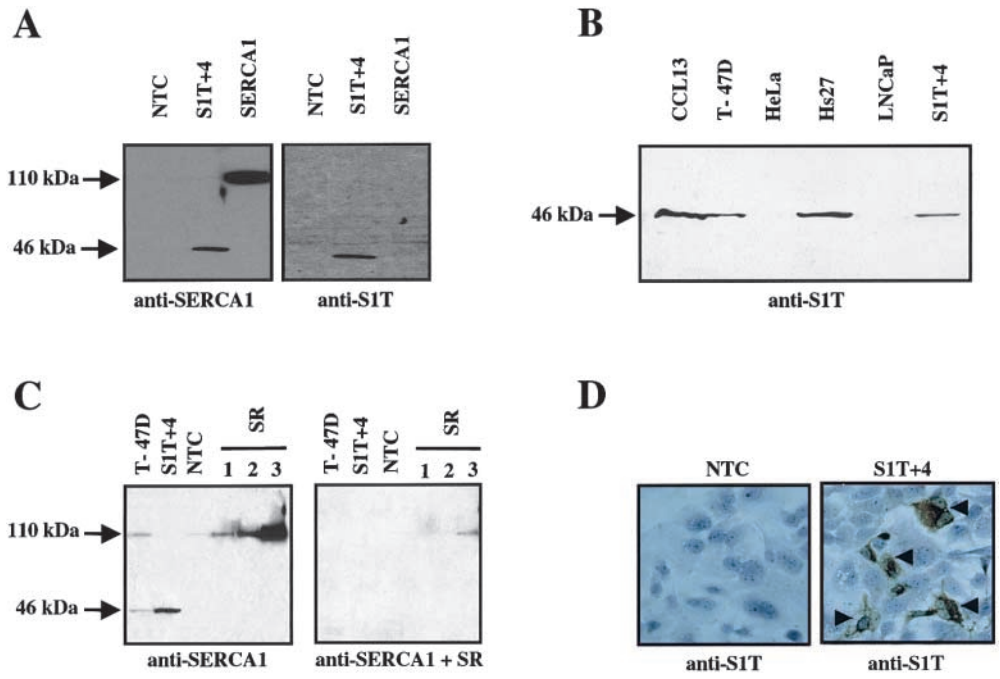


*Figure 3.* Detection of S1T+4 protein in transiently transfected HuH7 cells and nontransfected cell lines. (A) The same Western blot was successively hybridized with anti-SERCA1 antibody (79B) directed to the first cytoplasmic loop of SERCA1 and therefore recognizing both SERCA1 (110 kD) and S1T+4 (46 kD) proteins and with anti-S1T antibody directed to the S1T COOH-terminal 10 aa, which recognizes only S1T proteins. NTC, HuH7 nontransfected cells used as negative control. (B) Detection by Western blot analysis and anti-S1T antibody of S1T protein in HuH7 cells transiently transfected with S1T+4 (S1T+4), and in human nontransfected cell lines CCL13, T-47D, and Hs27, but not in HeLa and LNCaP. (C) Neutralization assay. (left) The microsomal fraction of the nontransfected T-47D cell line and of the HuH7 cell line transfected with the S1T+4 construct (S1T+4) was analyzed by Western blot using the anti-SERCA1 antibody 79B. SR (1, 3 ng; 2, 10 ng; and 3, 30 ng), purified sarcoplasmic reticulum from rabbit used as reference sample. (right) The membrane was dehybridized and rehybridized with the 79B antibody after its adsorption with the SR antigen (see Materials and Methods). Note the disappearing of SERCA1 and S1T bands in T-47D and in transfected HuH7 cells, and of the bands corresponding to 3 ng and 10 ng of SR. (D) A1T+4 transiently transfected HuII7 cells were analyzed by immunohistochemistry using anti-S1T antibody. Arrows indicate transfected cells.

vealed the S1T band (46 kD) in the T-47D nontransfected cell line and the HuH7 cell line transfected with the S1T+4 construct (S1T+4) as well as the SERCA1 band (110 kD) in the T-47D cell line and in the reference SR sample (Fig. 3 C, left). After dehybridization of the membrane and rehybridization with the 79B antibody, after its adsorption with SR antigen (see Materials and Methods), the SERCA1 and S1T bands in T-47D and transfected HuH7 cells disappeared, as well as the bands corresponding to 3 and 10 ng of SR (Fig. 3 C, right). This result shows the specificity of S1T protein detection in transfected and nontransfected cell lines. This test also led us to observe that, in the T-47D cell line (Fig. 3 C, left), the amount of expressed SERCA1 and S1T isoforms is similar.

The ER localization of S1T was assessed using two complementary approaches: immunolabeling and scanning confocal microscopy analysis. Immunohistochemistry and immunofluorescence performed on S1T+4-transfected cells with anti-S1T antibody showed a reticular signal consistent with S1T+4 localization to the ER (Fig. 3 D). Similar results were obtained using cells transfected with S1T+4 and S1T−4 fused to the myc tag and immunofluorescence using anti-myc antibody (data not shown).

To confirm this observation, we used scanning confocal microscopy analysis of HuH7 cells transfected with the SERCA1–GFP- and S1T+4–GFP-expressing vectors. Endogenous SERCA2b expression was revealed by the anti-SERCA2 monoclonal antibody and provided evidence for the expected colocalization of SERCA1 and SERCA2 proteins (Fig. 4 A). In contrast, SERCA1 was not found to colocalize with the mitochondrial reticulum (Fig. 4 C), which has been reported to be in close contact with the ER (Rizzuto et al., 1998). Our results also showed that S1T+4 colocalizes with SERCA2b (Fig. 4 B) but not with mitochondria (Fig. 4 D). This study made two important findings: (1) that S1T proteins are localized to the ER membrane and (2) that their localization may favor their interaction with the endogenous SERCA2b calcium pump.

### *S1T Proteins Reduce the Steady State Level of ER Calcium*

Since S1T proteins are localized to the ER membrane, we investigated whether they could modify the ER $Ca^{2+}$ content ($[Ca^{2+}]_{er}$) despite the fact that they are unable to pump calcium. To this aim, we used the erAEQ as a calcium probe. Cotransfection of erAEQ cDNA– and cDNA-encoding S1T+4 or S1T−4 was performed in HuH7, CCL13, and HeLa cells. To obtain a quantitative estimation of $[Ca^{2+}]_{er}$ values, the ER $Ca^{2+}$ concentration was reduced during the phase of erAEQ reconstitution with coelenterazine and the subsequent initial phase of perfusion (see Materials and Methods). Under these conditions, $[Ca^{2+}]_{er}$ was <10 μM. When calcium in the perfusion medium was switched to 1 mM, $[Ca^{2+}]_{er}$ level rose gradually to reach a plateau value (steady state level). In HuH7 cells cotransfected with erAEQ and S1T+4 or S1T−4, the plateau value was significantly lower 72 h after transfection (174 ± 58 μM, $n = 10$, $p$-value < 0.01, and 241 ± 78 μM, $n = 8$, $p$-value < 0.05, respectively) than that seen in control cells only transfected with erAEQ (330 ± 72 μM, $n = 14$) (Fig. 5 A and Table I). Taking the $[Ca^{2+}]_{er}$ of

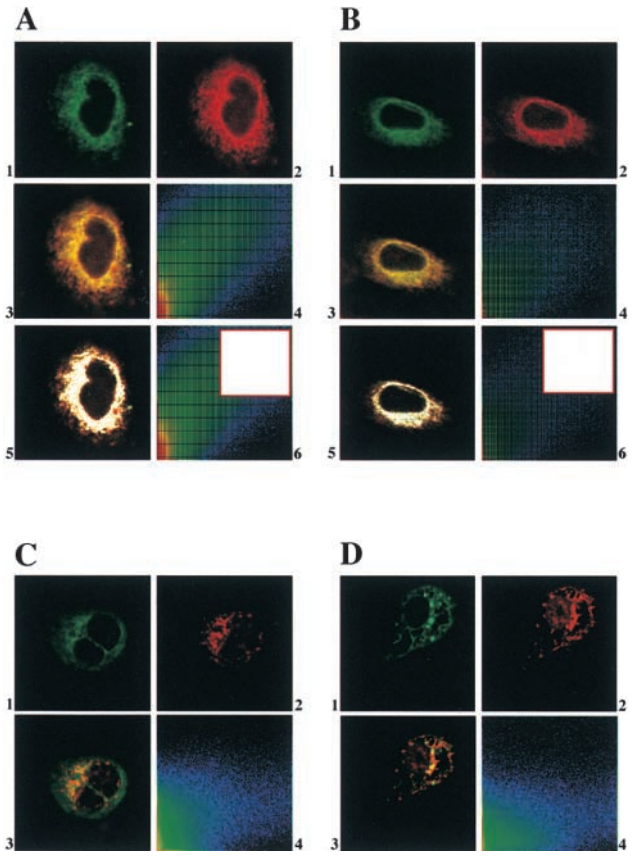


*Figure 4.* S1T+4 protein colocalizes with SERCA2b in the ER membrane. HuH7 cells transiently transfected with GFP fusion constructs, SERCA1–GFP (A 1 and C 1) or S1T+4–GFP (B 1 and D 1), were immunolabeled with anti-SERCA2 monoclonal antibody (clone IID8) (A 2 and B 2) or with antimitochondria E2 protein polyclonal antibody (anti-mito) (C 2 and D 2) and cyanin 5–coupled secondary antibody. Merging of the two signals (A 3, B 3, C 3, and D 3) and the cytofluorograms (obtained by plotting each green fluorescence point of the cell on the x axis and each red fluorescence point on the y axis) demonstrate the colocalization of SERCA1 and S1T+4 with endogenous SERCA2b (A 4 and B 4) in the ER membrane, but not with mitochondria (C 4 and D 4). Colocalization is indicated by the white points (A 5 and B 5) corresponding to the cytofluorogram white area with strongest colocalizing green and red fluorescence (A 6 and B 6).

control cells as 100%, the ER calcium steady state level was reduced to 53% in S1T+4 and to 73% in S1T−4 transfected cells. This effect was also found 48 h after transfection with the S1T+4 construct, the plateau value being reduced to 56% in transfected cells ($n = 11$, $p$-value $< 0.01$) as compared with control cells ($n = 10$).

In HeLa cells cotransfected with erAEQ and S1T+4 or S1T−4, the plateau value was also significantly lower (269 ± 33 μM, $n = 14$; $p$-value $< 0.01$, and 287 ± 44 μM, $n = 9$, $p$-value $< 0.01$, respectively) than that seen in control cells (400 ± 48 μM, $n = 7$) (Fig. 5 B and Table II) 48 h after transfection. In fact, taking the $[Ca^{2+}]_{er}$ of control cells as 100%, the ER calcium steady state level was reduced to 67% in S1T+4 and 72% in S1T−4-transfected cells. Similar results were obtained with CCl13 cells (data not shown). These results demonstrate that S1T proteins reduce $[Ca^{2+}]_{er}$ levels in three different cell lines.

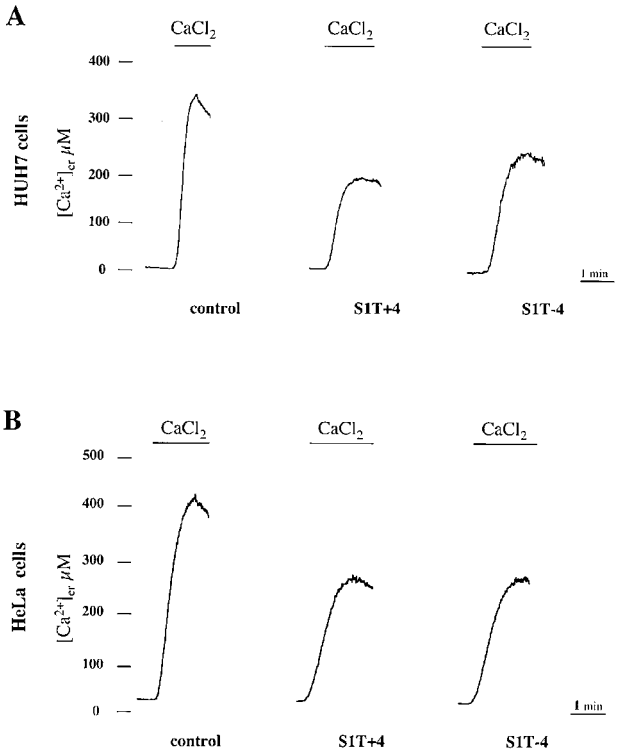


*Figure 5.* S1T proteins reduce the ER calcium content. $[Ca^{2+}]_{er}$ measurements were performed in HuH7 cells (A) and in HeLa cells (B) transfected with erAEQ (control), cotransfected with erAEQ and S1T+4 (S1T+4), or cotransfected with erAEQ and S1T−4 (S1T−4). Parallel batches of HeLa or HuH7 cells were analyzed 48 and 72 h after transfection, respectively. To obtain a quantitative estimation of $[Ca^{2+}]_{er}$, $[Ca^{2+}]$ was reduced during reconstitution of the aequorin with *n*-coelenterazine and the subsequent initial phase of perfusion. Where indicated, cells were perfused with 1 mM $CaCl_2$ solution ($CaCl_2$) until the plateau level was reached. Aequorin lumeniscence was collected and calibrated into $[Ca^{2+}]$ values.

### *S1T Proteins Reverse SERCA1 and SERCA2b-related Increase in the ER Calcium Content*

To investigate the effect of S1T in a context of increased ER calcium pumping, we overexpressed SERCA1, or the ubiquitous SERCA2b, in HuH7 and HeLa cells. HuH7 cells overexpressing SERCA1 or SERCA2b proteins showed a significantly higher steady state ER calcium level than controls (448 ± 81 μM, $n = 13$, $p$-value $< 0.01$, and 687 ± 105 μM, $n = 6$, $p$-value $< 0.01$, respectively, vs. 330 ± 72 μM, $n = 14$) (Fig. 6, A and B, and Table I). Cotransfection of SERCA1 and S1T+4 or S1T−4 significantly reduced $[Ca^{2+}]_{er}$ to 297 ± 78 μM, $n = 11$, $p$-value $<$ 0.01, and 343 ± 99 μM, $n = 10$, $p$-value $= 0.02$), respectively (Table I). Cotransfection of SERCA2b and S1T+4 or S1T−4 also significantly reduced $[Ca^{2+}]_{er}$ to 434 ± 131 μM, $n = 4$, $p$-value $< 0.01$, and 445 ± 61 μM, $n = 4$, $p$-value $< 0.01$, respectively (Table I). Similar results were obtained in HeLa cells transfected with SERCA1 (446 ± 59 μM, $n = 8$) and SERCA1+S1T+4 (329 ± 55 μM, $n = 4$, $p$-value $< 0.05$) or SERCA1+S1T−4 (327 ± 59 μM, $n = 4$, $p$-value $< 0.05$) (Fig. 6 C and Table II).

In our system, SERCA2b induced a higher steady state ER calcium level than SERCA1. This result may be due to

*Table I. Analysis of Steady State [$Ca^{2+}$] Levels in the ER of Transiently Transfected HuH7 Cells*

| Constructs | ER [$Ca^{2+}$] ± SEM | *p*-value | *n* | % ER [$Ca^{2+}$]* |
|---|---|---|---|---|
| | *μM* | | | |
| Control | 330 ± 72 | | 14 | 100 |
| S1T+4 | 174 ± 58 | <0.01‡ | 10 | 53 |
| S1T−4 | 241 ± 78 | <0.05‡ | 8 | 73 |
| SERCA1 | 448 ± 81 | <0.01‡ | 13 | 136 |
| SERCA1 + S1T+4 | 297 ± 78 | <0.01§ | 11 | 90 |
| SERCA1 + S1T−4 | 343 ± 99 | 0.02§ | 10 | 103 |
| SERCA2 | 678 ± 105 | <0.01‡ | 6 | 208 |
| SERCA2 + S1T+4 | 434 ± 131 | <0.01‖ | 4 | 131 |
| SERCA2 + S1T−4 | 445 ± 61 | <0.01‖ | 4 | 134 |

Mean ± SEM. *n*, total number of erAEQ measurement tests.
*Evaluation of ER $Ca^{2+}$ loading as compared to that of nontransfected cells, considered as reference (100%).
‡Versus control.
§Versus SERCA1.
‖Versus SERCA2.

the different type (pig versus human) of ATPase used and/or to the type of promoter (SV-40 versus CMV).

### *Endogenous SERCA2b Expression Is Not Modified by the Overexpression of S1T*

Although S1T are unable to pump calcium, they could, in theory, downregulate the endogenous SERCA2b expression, thus reducing ER calcium loading. To address this question, COS cells were transfected with S1T+4-expressing vector, and Western blot analysis was carried out on the microsomal fraction of S1T+4 transiently transfected cells and nontransfected cells. The expression of endogenous SERCA2b was detected using the anti-SERCA2 monoclonal antibody. Although ≥60% of COS cells expressed S1T+4 (assessed by cotransfection with GFP empty vector), no major differences in SERCA2b expression were observed repeatedly in transfected as compared with nontransfected cells (Fig. 7 A). Consistent results were obtained with HuH7 cells, in which transfection efficiency was lower (∼40%). Thus, the reduced ER calcium loading due to overexpression of S1T is not related to a sound downregulation of endogenous SERCA2b expression.

### *S1T Proteins Increase Calcium Leakage from the ER*

An alternative mechanism leading to reduced $[Ca^{2+}]_{er}$ in S1T-overexpressing cells may be an increased rate of calcium leakage from the ER. It is well established that the rates of calcium uptake and release are equal in the steady state. Thus, the rate of $[Ca^{2+}]_{er}$ decrease upon the blockade of SERCA should reflect the rate of $Ca^{2+}$ cycling across the ER membrane and the leakage rate at any given steady state $[Ca^{2+}]_{er}$ (Pinton et al., 2000). Fig. 7 B shows the relationship between the $[Ca^{2+}]_{er}$ value and the leakage rate, which could be fitted using a power equation. There is a clear profile of faster $Ca^{2+}$ efflux in S1T+4- and S1T−4-overexpressing HuH7 cells than in control cells, for the majority of $[Ca^{2+}]_{er}$ values. Fig. 7 C shows three overlapping curves obtained from HuH7 cells nontransfected (control) and transfected with the S1T+4 or S1T−4 construct, having comparable steady state calcium levels. The kinetics of $Ca^{2+}$ efflux is clearly more rapid in S1T-transfected than in nontransfected cells. Consistent results were obtained in S1T+4- and S1T−4-overexpressing HeLa cells (data not shown).

*Table II. Analysis of Steady State [$Ca^{2+}$] Levels in the ER of Transiently Transfected HeLa Cells*

| Constructs | ER [$Ca^{2+}$] ± SEM | *p*-value | *n* | % ER [$Ca^{2+}$]* |
|---|---|---|---|---|
| | *μM* | | | |
| Control | 400 ± 48 | | 7 | 100 |
| S1T+4 | 269 ± 33 | <0.01‡ | 14 | 67 |
| S1T−4 | 287 ± 44 | <0.05‡ | 9 | 72 |
| SERCA1 | 446 ± 59 | NS‡ | 8 | 112 |
| SERCA1+ S1T+4 | 329 ± 55 | <0.05§ | 4 | 82 |
| SERCA1 + S1T−4 | 327 ± 59 | <0.05§ | 4 | 82 |

Mean ± SEM. *n*, total number of erAEQ measurement tests.
*Evaluation of ER $Ca^{2+}$ loading as compared to that of nontransfected cells, considered as reference (100%).
‡Versus control.
§Versus SERCA1.

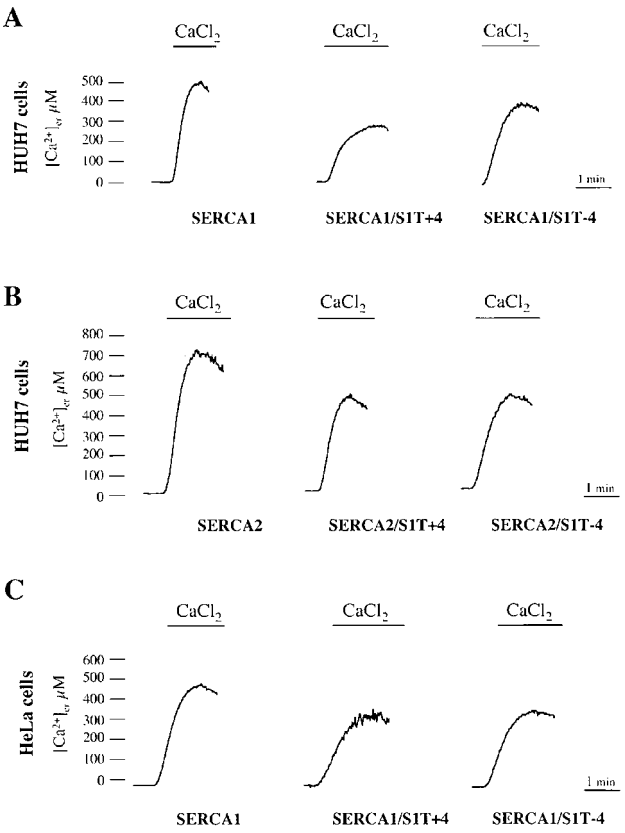


*Figure 6.* S1T proteins reverse SERCA1- and SERCA2b-induced increases of $[Ca^{2+}]_{er}$. HuH7 (A and B) and HeLa (C) cells were cotransfected with erAEQ and SERCA1 (A and C) or SERCA2b (B). Cotransfection of erAEQ, SERCA1, or SERCA2b and S1T constructs was carried out as described in Materials and Methods. Quantitative assessment of $[Ca^{2+}]_{er}$ was performed as described in the legend to Fig. 5.

### *S1T Proteins Are Expressed as Dimers*

The question has been raised as to the mechanism through which S1T overexpression increases ER $Ca^{2+}$ leakage. Two possibilities were considered: (1) that the direct binding of S1T to endogenous SERCA would partially block

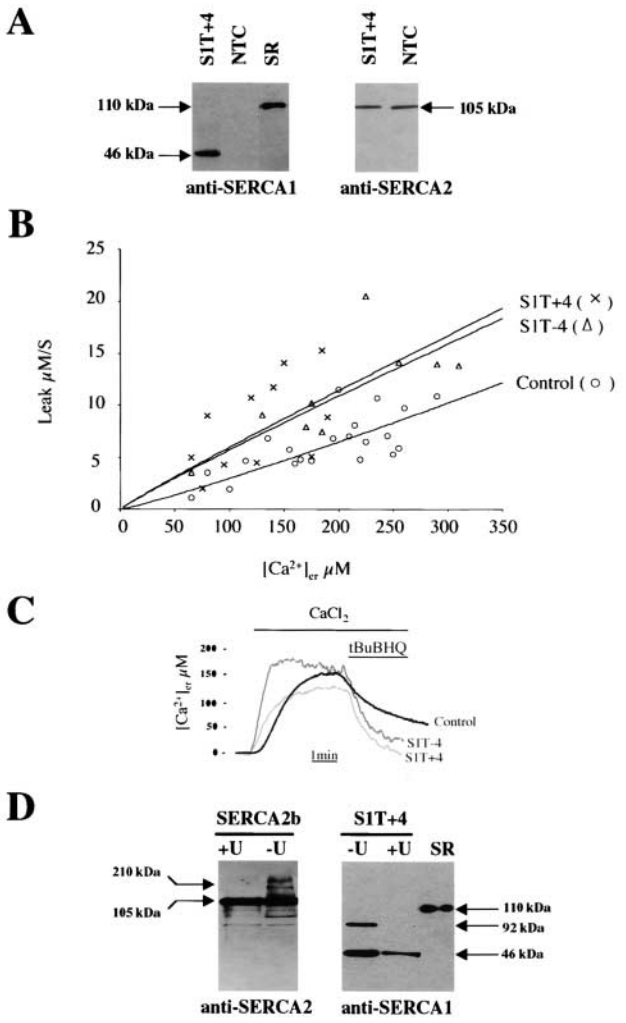


*Figure 7.* Expression of endogenous SERCA2b in cells overexpressing S1T (A), relationship between $[Ca^{2+}]_{er}$ and leakage rate in control cells, S1T+4-, and S1T−4-expressing cells (B and C), and dimerization of S1T+4 proteins under mildly denaturing conditions (D). (A) Expression of endogenous SERCA2b is similar in S1T+4-transfected as compared with nontransfected cells. Western blot analysis of the microsomal fraction of S1T+4 transiently transfected and nontransfected COS7 cells. The same extracts were run in parallel (SDS-PAGE). Corresponding membranes were hybridized with anti-SERCA1 (79B) and anti-SERCA2 (IID8) antibodies. (B) S1T proteins increase ER calcium leakage from the ER. Dependence on $[Ca^{2+}]_{er}$ of the $Ca^{2+}$ leak rate from the ER. Transfection, depletion of $Ca^{2+}$ stores, and aequorin reconstitution were carried out as described in the legend to Fig. 5; after the steady state $[Ca^{2+}]_{er}$ was reached, $Ca^{2+}$ release was initiated by treating the cells with 50 μM tBuBHQ. Based on the experimental trace, the maximum rates of $Ca^{2+}$ release (measured from the first derivative) at different $[Ca^{2+}]_{er}$ values were calculated and plotted for S1T-transfected and control cells. The plot contains data obtained from independent experiments ($n$ = 21 for controls, $n$ = 9 for S1T−4, and $n$ = 11 for S1T+4). Due to the mixing time in the luminometer chamber, the kinetics of $[Ca^{2+}]_{er}$ decrease are sigmoidal, and the maximum rate is obtained 2–3 s after the addition of tBuBHQ. Accordingly, we considered the maximum rates as the best approximation for the initial rate of $[Ca^{2+}]_{er}$ reduction. Fitting of the curve was performed using Microsoft Excel software. (C) $[Ca^{2+}]_{er}$ measurements performed in HuH7 cells nontransfected (control) and transfected with the S1T+4 or S1T−4 construct, having comparable steady state calcium levels. The kinetics of $Ca^{2+}$ efflux is clearly more rapid in S1T-transfected than in nontransfected cells. (D) S1T+4 proteins form dimers (92 kD) under mildly denaturing conditions. HuH7 cells were transiently transfected with S1T+4- (right) and SERCA2b-expressing (left) constructs. Western blots were performed with heated samples treated (+U) or not (−U) with urea. A 92-kD band corresponding to S1T+4 dimers was detected for the S1T+4 sample without urea treatment (−U). Note the absence of a 151-kD band that would have been consistent with heterodimers S1T+4–SERCA2b. A 210-kD band corresponding to SERCA2b dimers was present in the SERCA2b sample without urea (−U). SR, see legend to Fig. 3.

ATPase activity, thus enhancing ER $Ca^{2+}$ leakage; and (2) that the faster rate of $Ca^{2+}$ efflux from the ER is due to a cation channel formed by S1T dimers or aggregates. To investigate these two possibilities, we performed a Western blot analysis under mild denaturing conditions (heated sample without urea) (Soulié et al., 1996). Under these conditions, a relevant proportion of S1T+4 was found to form homodimers (92 kD) (Fig. 7 D). By comparison, a far smaller proportion of SERCA2b was shown to form homodimers. We also noticed that, during repeated analyses, no heterodimers formed by SERCA2b and S1T+4 (expected size 151 kD) could be detected (Fig. 7 D, right). Although we cannot exclude S1T aggregates and/or multidimers in native conditions, they are not visible using mild denaturing conditions. This finding indicates that, if S1T aggregates and/or multidimers exist under native conditions, their stability is lower than that of homodimers. In this setting, the existence of multihomodimers in native conditions would be more plausible than that of S1T aggregates. Thus, the simplest explanation for the increase in ER $Ca^{2+}$ leakage is the formation of a cation channel, in the ER membrane, by the dimerization of S1T proteins. Indeed, each S1T monomer has a calcium-binding residue (Glu-309), which, along with additional residues, in particular Glu-58 and Gln-108, could participate to create a calcium-binding site in the new protein conformation, and a cation channel in the case of S1T dimerization.

### *Overexpression of S1T Proteins Induces Apoptosis*

In a previous report, we showed that the overexpression of Hepatitis B virus–SERCA1 chimeric transcripts (with exon 4 and/or exon 11 splicing) induces apoptosis and that this effect is due to both the viral and SERCA moieties of chimeric proteins (Chami et al., 2000). Along the same line, we investigated whether S1T overexpression could be associated with apoptotic cell death. Apoptosis was assessed using two complementary approaches. Morphological analysis was based on counting of the number of apoptotic bodies in cells expressing GFP fusion proteins (see Materials and Methods). Using this method, we carried out preliminary tests 48, 72, and 96 h after transfection in order to define the suitable time window for assessment of apoptosis. As compared with nontransfected cells and cells transfected with empty vector, S1T transfected cells showed a significant proportion of apoptotic cells 72 h after transfection, but not before. Both S1T+4-GFP and S1T−4-GFP significantly induced apoptosis (16.5% for S1T+4, $p$-value $< 0.0001$, and 25.5% for S1T−4, $p$-value $<$

0.0001) in HuH7 cells, compared with the empty GFP vector used as control (5.2%). The percentage of apoptotic cells in SERCA1- and SERCA2-overexpressing cells was not significantly higher than that seen in control cells (7%, $p = 0.029$, for SERCA1, and 7%, $p = 0.09$, for SERCA2b) (Fig. 8 A). Similar results were obtained with CCL13 cells (data not shown).

Flow cytometry analysis of apoptosis was performed in HepG2 cells, based on alteration in the mitochondrial structure assessed by NAO staining. S1T+4- and S1T−4-transfected cells showed a significantly higher number of apoptotic cells, characterized by smaller cell size associated with a lower incorporation of NAO (22%, $p$-value $< 0.001$, and 21%, $p$-value $< 0.0019$, respectively), compared with the controls: nontransfected cells (11%) and pcDNA3-transfected cells (6%) (Fig. 8 B). From these experiments we conclude that overexpression of S1T proteins induces apoptosis in three different cell lines (CCL13, HuH7, and HepG2).

## *Discussion*

We describe for the first time that SERCA1 truncated proteins encoded by new splice variants (S1T) of the SERCA1 gene. S1T are characterized by exon 4 and/or exon 11 splicing, leading to COOH-terminally truncated proteins with deletion of transmembrane segments M2 and/or M5 to M10 including six out of seven transmembrane calcium-binding residues (Toyoshima et al., 2000). Consistent with the analysis of previously reported SERCA1 mutants (MacLennan et al., 1998), they are unable to pump calcium. We show that S1T protein overexpression is associated with a reduction in the ER $Ca^{2+}$ steady state level and an increase in ER $Ca^{2+}$ leakage. Our results also demonstrate that these proteins modulate SERCA-dependent ER calcium accumulation and induce apoptotic cell death.

S1T splice variants were detectable by RT-PCR at variable levels in different adult tissues, including spleen, thymus, pancreas, kidney, and liver, but not in adult and fetal skeletal muscle and heart. The relative amount of S1T, as compared with SERCA1 transcripts, differed as a function of the tissues analyzed, and was higher in fetal liver, kidney, and brain than in the corresponding adult tissues. These observations were consistent with a switch from SERCA1 to S1T expression in fetal cells. We detected, by using Western Blot analysis, the expression of S1T+4 protein in human nontransfected cell lines T-47D, CCL13, and Hs27 and confirmed the specificity of these results by the antigen–antibody competition test. In contrast, S1T proteins were not detectable in nontransfected HeLa and LNCaP cell lines. Therefore, S1T proteins were detected in a primary (Hs27) and two (T-47D and CCL13) out of four analyzed transformed cells. Together, our results are consistent with the view that S1T proteins can exert a biological tightly regulated function.

Using confocal microscopy, S1T were shown to colocalize with SERCA2b into the ER membrane. This localization was also predicted by structural analysis of S1T. Indeed, they retain the $NH_2$-terminal 28 residues previously identified as being the minimal SERCA1 ER targeting signal (Guerini et al., 1998), and S1T+4 was also found to

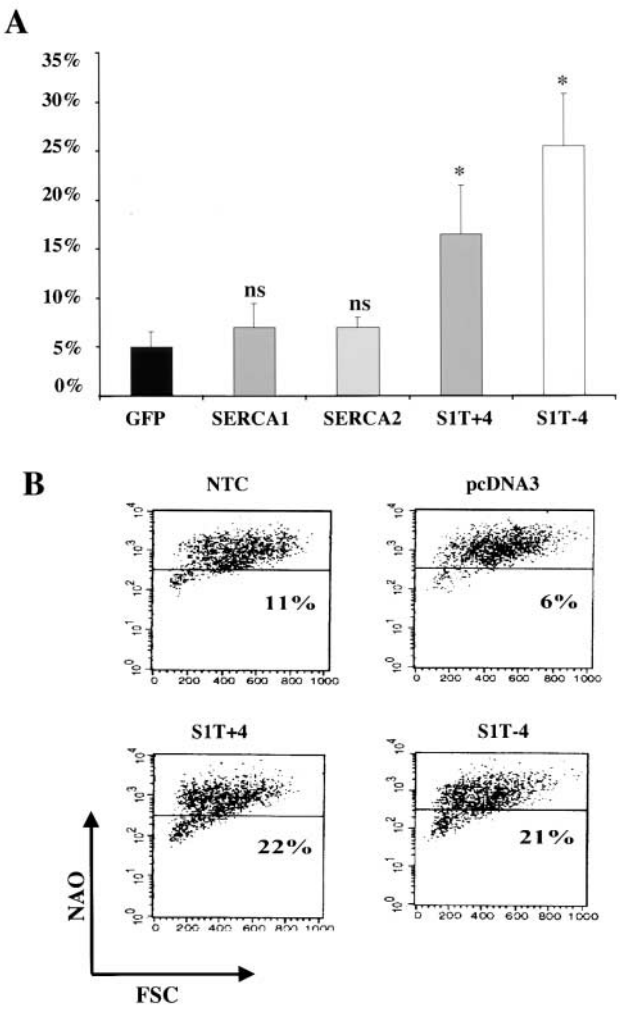


*Figure 8.* S1T proteins overexpression induce apoptosis. (A) Morphological assessment of apoptotic bodies in HuH7 cells transfected with GFP empty vector (GFP), SERCA1–GFP (SERCA1), and SERCA2-GFP (SERCA2), as controls and in cells transfected with S1T+4–GFP or S1T−4–GFP fusion constructs. Apoptotic bodies were recorded among ≥600 transfected cells in at least three independent experiments. NS, not significant, *$p$-value $< 0.0001$ calculated versus GFP-transfected cells. (B) FACScan® analysis of apoptosis by mitochondrial incorporation of NAO (ordinates) and cell size (abscisses) in nontransfected HepG2 cells (NTC), cells transfected with S1T+4 and S1T−4 constructs, and empty vector (pcDNA3). The percentage of apoptotic cells is defined by lower NAO incorporation associated with a smaller cell size.

have the first four transmembrane domains (M1 to M4) that act as the signal anchor and stop transfer sequence (Bayle et al., 1997). The structure of S1T−4 is unpredictable, since this protein also lacks the five COOH-terminal residues of M1 and the complete M2 transmembrane domain. Consequently, it is difficult to clarify the orientation of the following M3 and M4 in the ER membrane. However, our results indicate that S1T−4 also localizes to the ER membrane. This result is supported by previous findings showing that the chimeric protein Xt/St-4, which, when compared with S1T−4, has the $NH_2$-terminal

SERCA1 51 residues replaced by 148 viral residues, is targeted to the ER (Chami et al., 2000).

We have shown that the in vitro expression of S1T reduces the ER calcium content by 30–50% in three different cell lines. We have also shown that this reduction was induced in a context of ER calcium overload due to SERCA1 or SERCA2b overexpression. This demonstrates that S1T expression can modulate SERCA-dependent calcium accumulation. Several mechanisms may be involved in this effect. Endogenous SERCA2b expression might be downregulated by the overexpression of S1T. Although we cannot rule out extremely low levels of downregulation, our Western blot studies did not evidence such downregulation, which therefore is unlikely to be a major mechanism. On the other hand, the rate of $Ca^{2+}$ efflux in S1T-overexpressing cells was clearly faster than in control cells and thus S1T expression increases the $Ca^{2+}$ leakage from the ER. A possible explanation is that S1T proteins bind the endogenous SERCA2b and partially block its pumping activity. This direct interaction is possible since SERCA proteins have been shown to form aggregates (Martonosi, 1996). However, Western blot analyses of S1T transiently transfected cells, performed in mild denaturing conditions (heated samples without urea), failed to demonstrate heterodimers of S1T with endogenous SERCA2b proteins. In contrast, homodimers of S1T were easily and clearly detected, at higher proportions than SERCA2b homodimers. Actually, the truncation of S1T allows several residues of M2, M3, and M4, interacting with M5 and M6 residues in SERCA1a (see Figure 3 a in Toyoshima et al., 2000), to be in contact with the ER membrane lipids, and therefore in a thermodynamic unfavorable state. This is particularly critical for the C=O and NH of residues Ile-307 to Gly-310 in M4, which are unwound (i.e., non–α helical), and predictably not H-bonded when they are in contact with the lipid hydrophobic region. In this setting, S1T homodimers, allowing these residues to be H bonded, appear as a more stable conformation. Thus, although it is difficult to completely exclude the possibility of a direct S1T–SERCA2b interaction blocking the endogenous ATPase, it is clear that S1T homodimers are more stable than heterodimers in HuH7-transfected cells and that their presence, in native conditions, is plausible.

Taking into account the fact that M4 is still present in S1T proteins and contains four of the six calcium-binding residues of calcium-binding site II (Fig. 1 B), it is reasonable to hypothesize that S1T homodimers may form a cation channel. Due to the structural modifications of the truncated proteins in respect to SERCA1, it is also possible that such a channel may involve negatively charged residues that could contribute to the increase of ER $Ca^{2+}$ leakage. Glu-58 in M1 and Gln-108 in M2 (Fig. 1 D), which are located close to Glu-309, are good candidates to play this role.

We demonstrated that S1T overexpression induces apoptosis in three different cell lines, as determined by the counting of apoptotic bodies and by FACS® analysis of the mitochondrial structure using NAO incorporation. Several reports have shown that SERCA inhibition by different compounds and mechanisms (thapsigargin, tBuBHQ, and cyclopiazonic acid) is followed by apoptosis (Furuya et al., 1994; Zhu and Loh, 1995; Preston et al., 1997; Zhou et al., 1998; Wertz and Dixit, 2000). In these models, SERCA inhibition induced $[Ca^{2+}]_{er}$ depletion associated with capacitative calcium entry and an increase in cytosolic free calcium concentration ($[Ca^{2+}]_c$). In certain experimental systems, the perturbation of calcium homeostasis in both cell compartments has been associated with apoptotic cell death (Bian et al., 1997; Skryma et al., 2000). Other reports have shown, however, that ER depletion alone was sufficient to induce apoptosis (Furuya et al., 1994; He et al., 1997; Zhou et al., 1998; Wertz and Dixit, 2000). ER calcium depletion induced by the overexpression of S1T was found in HuH7 cells 48 and 72 h after transfection, whereas a significant number of apoptotic bodies was detected in the same cells 72 h, but not 48 h, after transfection. In this context, S1T-induced ER calcium depletion might play a role in apoptosis of transfected cells, although we cannot rule out that S1T may lead to apoptosis by means of a mechanism that differs from a reduction in the ER calcium pool. In fact, a reduction in the ER calcium content has been described in HeLa (Pinton et al., 2000) and HEK (Foyouzi-Youssefi et al., 2000) cells overexpressing the antiapoptotic protein Bcl2. Furthermore, ER calcium depletion in lymphoid cells has been associated with a delay in glucocorticoid-induced apoptosis (Distelhorst and McCormick, 1996). Differences in experimental conditions, cell type, and the degree of ER calcium reduction may explain the contrasting results reported concerning the relationship between reduced ER calcium pool, apoptosis, and expression of antiapoptotic proteins.

SERCA proteins are critical regulatory components of $Ca^{2+}$ signaling. On the one hand, by transporting cytosolic $Ca^{2+}$ against a concentration gradient into the lumen of the ER, they represent a relevant factor that controls $Ca^{2+}$ signals in the cytosol (Berridge et al., 1998). It has been shown that SERCA genes control the IP3-mediated calcium waves (Camacho and Lechleiter, 1993), the amplitude and duration of which differentially activate certain transcription factors (Dolmetsch et al., 1997). On the other hand, SERCA proteins also control the free calcium level in the ER, which is involved in basic cellular processes such as protein synthesis, folding, and stress response (Meldolesi and Pozzan, 1998). In this setting, it is conceivable that the whole process of $Ca^{2+}$ accumulation into and release from the ER has to be finely tuned. Indeed, SERCA2a and SERCA1 pump activities have been shown to be modulated, in muscle cells, by phospholamban, which undergoes a physical interaction with SERCA transmembrane domain M6 (Asahi et al., 2000). In fast-twitch skeletal muscle cells, sarcolipin interacts with SERCA1 and inhibits $Ca^{2+}$ uptake in a $Ca^{2+}$-dependent manner (Odermatt et al., 1998). SERCA2b may also be inhibited by a physical interaction with phosphorylated calnexin, a transmembrane ER chaperone. It has been shown that IP3-induced $Ca^{2+}$ release results in calnexin dephosphorylation and SERCA derepression (Roderick et al., 2000). Our results now provide evidence for a further mechanism modulating ER $Ca^{2+}$ loading in nonmuscle cells.

In conclusion, our work describes new truncated SERCA1 proteins, which are unable to pump calcium and display a dominant negative biological effect on SERCA-dependent ER calcium accumulation. It reveals a previously unknown mechanism involved in ER calcium ho-

meostasis and may constitute a new tool to study the physiological role of SERCA proteins in calcium signaling and control of cell death.

We wish to thank P. Champeil for helpful discussion.

This work was supported by grants from The French Institute of Health and Medical Research (INSERM). Mounia Chami is recipient of fellowships from the National League Against Cancer and the Foundation for Medical Research. Devrim Gozuacik is recipient of fellowships from the Association for Research Against Cancer.

Submitted: 27 November 2000
Revised: 22 March 2001
Accepted: 2 April 2001

### *References*

Asahi, M., E. McKenna, K. Kurzydlowski, M. Tada, and D.H. MacLennan. 2000. Physical interactions between phospholamban and sarco(endo)plasmic reticulum $Ca^{2+}$-ATPases are dissociated by elevated $Ca^{2+}$, but not by phospholamban phosphorylation, vanadate, or thapsigargin, and are enhanced by ATP. *J. Biol. Chem.* 275:15034–15038.

Bayle, D., D. Weeks, S. Hallen, K. Melchers, K. Bamberg, and G. Sachs. 1997. In vitro translation analysis of integral membrane proteins. *J. Recept. Signal Transduct. Res.* 17:29–56.

Berridge, M.J., M.D. Bootman, and P. Lipp. 1998. Calcium—a life and death signal. *Nature.* 395:645–648.

Bian, X., F.M. Hughes, Jr., Y. Huang, J.A. Cidlowski, and J.W. Putney, Jr. 1997. Roles of cytoplasmic $Ca^{2+}$ and intracellular $Ca^{2+}$ stores in induction and suppression of apoptosis in S49 cells. *Am. J. Physiol.* 272:C1241–C1249.

Brini, M., R. Marsault, C. Bastianutto, J. Alvarez, T. Pozzan, and R. Rizzuto. 1995. Transfected aequorin in the measurement of cytosolic $Ca^{2+}$ concentration ($[Ca^{2+}]c$). A critical evaluation. *J. Biol. Chem.* 270:9896–9903.

Brini, M., D. Bano, S. Manni, R. Rizzuto, and E. Carafoli. 2000. Effects of PMCA and SERCA pump overexpression on the kinetics of cell $Ca^{2+}$ signalling. *EMBO J.* 19:4926–4935.

Camacho, P., and J.D. Lechleiter. 1993. Increased frequency of calcium waves in *Xenopus laevis* oocytes that express a calcium-ATPase. *Science.* 260:226–229.

Caspersen, C., P.S. Pedersen, and M. Treiman. 2000. The sarco/endoplasmic reticulum calcium-ATPase 2b is an endoplasmic reticulum stress-inducible protein. *J. Biol. Chem.* 275:22363–22372.

Chami, M., D. Gozuacik, K. Saigo, T. Capiod, P. Falson, H. Lecoeur, T. Urashima, J. Beckmann, M.-L. Gougeon, M. Claret, et al. 2000. Hepatitis B virus-related insertional mutagenesis implicates SERCA1 gene in the control of apoptosis. *Oncogene.* 19:2877–2886.

Chelly, J., J.-P. Concordet, J.-C. Kaplan, and A. Kahn. 1989. Illegitimate transcription: transcription of any gene in any cell type. *Proc. Natl. Acad. Sci. USA.* 86:2617–2621.

De Smedt, H., J. Eggermont, F. Wuytack, J. Parys, L. Van Den Bosch, L. Missiaen, J. Verbist, and R. Casteels. 1991. Isoform switching of the sarco(endo)plasmic reticulum $Ca^{2+}$ pump during differentiation of BC3H1 myoblasts. *J. Biol. Chem.* 266:7092–7095.

Distelhorst, C.W., and T.S. McCormick. 1996. Bcl-2 acts subsequent to and independent of $Ca^{2+}$ fluxes to inhibit apoptosis in thapsigargin- and glucocorticoid-treated mouse lymphoma cells. *Cell Calcium.* 19:473–483.

Dolmetsch, R.E., R.S. Lewis, C.C. Goodnow, and J.I. Healy. 1997. Differential activation of transcription factors induced by $Ca^{2+}$ response amplitude and duration. *Nature.* 386:855–858 (erratum published 388:308).

Falson, P., T. Menguy, F. Corre, L. Bouneau, A.G. de Gracia, S. Soulie, F. Centeno, J.V. Moller, P. Champeil, and M. le Maire. 1997. The cytoplasmic loop between putative transmembrane segments 6 and 7 in sarcoplasmic reticulum $Ca^{2+}$-ATPase binds $Ca^{2+}$ and is functionally important. *J. Biol. Chem.* 272:17258–17262.

Foyouzi-Youssefi, R., S. Arnaudeau, C. Borner, W.L. Kelley, J. Tschopp, D.P. Lew, N. Demaurex, and K.H. Krause. 2000. Bcl-2 decreases the free $Ca^{2+}$ concentration within the endoplasmic reticulum. *Proc. Natl. Acad. Sci. USA.* 97:5723–5728.

Fuentes, J., A. Lompré, J. Moller, P. Falson, and M. le Maire. 2000. Clean Western blots of membrane proteins after yeast heterologous expression following a shortened version of the method of Perini et al. *Anal. Biochem.* 285: 276–278.

Furuya, Y., P. Lundmo, A. Short, D. Gill, and J. Isaacs. 1994. The role of calcium, pH, and cell proliferation in the programmed (apoptotic) death of androgen-independent prostatic cancer cells induced by thapsigargin. *Cancer Res.* 54:6167–6175.

Guerini, D., E. Garcia-Martin, A. Zecca, F. Guidi, and E. Carafoli. 1998. The calcium pump of the plasma membrane: membrane targeting, calcium binding sites, tissue-specific isoform expression. *Acta Physiol. Scand. Suppl.* 643: 265–273.

He, H., M. Lam, T.S. McCormick, and C.W. Distelhorst. 1997. Maintenance of calcium homeostasis in the endoplasmic reticulum by Bcl-2. *J. Cell Biol.* 138: 1219–1228.

Jolly, C., and R.I. Morimoto. 2000. Role of the heat shock response and molecular chaperones in oncogenesis and cell death. *J. Natl. Cancer Inst.* 92:1564–1572.

Kuo, T.H., H.R. Kim, L. Zhu, Y. Yu, H.M. Lin, and W. Tsang. 1998. Modulation of endoplasmic reticulum calcium pump by Bcl-2. *Oncogene.* 17:1903–1910.

Launay, S., M. Giann, T. Kovacs, R. Bredoux, A. Bruel, P. Gelebart, F. Zassadowski, C. Chomienne, J. Enouf, and B. Papp. 1999. Lineage-specific modulation of calcium pump expression during myeloid differentiation. *Blood.* 93: 4395–4405.

Lechleiter, J.D., L.M. John, and P. Camacho. 1998. $Ca^{2+}$ wave dispersion and spiral wave entrainment in *Xenopus laevis* oocytes overexpressing $Ca^{2+}$ ATPases. *Biophys. Chem.* 72:123–129.

Lee, M., X. Xu, W. Zeng, J. Diaz, T. Kuo, F. Wuytack, L. Racymaekers, and S. Muallem. 1997. Polarized expression of $Ca^{2+}$ pumps in pancreatic and salivary gland cells. Role in initiation and propagation of $(Ca^{2+})i$ waves. *J. Biol. Chem.* 272:15771–15776.

Lytton, J., M. Westlin, S.E. Burk, G.E. Shull, and D.H. MacLennan. 1992. Functional comparisons between isoforms of the sarcoplasmic or endoplasmic reticulum family of calcium pumps. *J. Biol. Chem.* 267:14483–14489.

Ma, T., D. Mann, J. Lee, and G. Gallinghouse. 1999. SR compartment calcium and cell apoptosis in SERCA overexpression. *Cell Calcium.* 26:25–36.

MacLennan, D.H., W.J. Rice, and N.M. Green. 1997. The mechanism of $Ca^{2+}$ transport by sarco(endo)plasmic reticulum $Ca^{2+}$-ATPases. *J. Biol. Chem.* 272:28815–28818.

MacLennan, D.H., W.J. Rice, A. Odermatt, and N.M. Green. 1998. Structure-function relationships in the $Ca^{2+}$-binding and translocation domain of SERCA1: physiological correlates in Brody disease. *Acta Physiol. Scand. Suppl.* 643:55–67.

Martin, V., R. Bredoux, E. Corvazier, B. Papp, and J. Enouf. 2000. Platelet $Ca^{2+}$-ATPases: a plural, species-specific, and multiple hypertension-regulated expression system. *Hypertension.* 35:91–102.

Martonosi, A.N. 1996. Structure-function relationships in the $Ca^{2+}$-ATPase of sarcoplasmic reticulum: facts, speculations and questions for the future. *Biochim. Biophys. Acta.* 1275:111–117.

Maruyama, K., and D.H. MacLennan. 1988. Mutation of aspartic acid-351, lysine-352, and lysine-515 alters the $Ca^{2+}$ transport activity of the $Ca^{2+}$-ATPase expressed in COS-1 cells. *Proc. Natl. Acad. Sci. USA.* 85:3314–3318.

Meldolesi, J., and T. Pozzan. 1998. The endoplasmic reticulum $Ca^{2+}$ store: a view from the lumen. *Trends Biochem. Sci.* 23:10–14.

Menguy, T., F. Corre, L. Bouneau, S. Deschamps, J.V. Moller, P. Champeil, M. le Maire, and P. Falson. 1998. The cytoplasmic loop located between transmembrane segments 6 and 7 controls activation by $Ca^{2+}$ of sarcoplasmic reticulum $Ca^{2+}$-ATPase. *J. Biol. Chem.* 273:20134–20143.

Montero, M., M. Brini, R. Marsault, J. Alvarez, R. Sitia, T. Pozzan, and R. Rizzuto. 1995. Monitoring dynamic changes in free $Ca^{2+}$ concentration in the endoplasmic reticulum of intact cells. *EMBO J.* 14:5467–5475.

Odermatt, A., S. Becker, V.K. Khanna, K. Kurzydlowski, E. Leisner, D. Pette, and D.H. MacLennan. 1998. Sarcolipin regulates the activity of SERCA1, the fast-twitch skeletal muscle sarcoplasmic reticulum $Ca^{2+}$-ATPase. *J. Biol. Chem.* 273:12360–12369.

Petit, P.X., H. Lecoeur, E. Zorn, C. Dauguet, B. Mignotte, and M.L. Gougeon. 1995. Alterations in mitochondrial structure and function are early events of dexamethasone-induced thymocyte apoptosis. *J. Cell Biol.* 130:157–167.

Pinton, P., D. Ferrari, P. Magalhaes, K. Schulze-Osthoff, F. Di Virgilio, T. Pozzan, and R. Rizzuto. 2000. Reduced loading of intracellular $Ca^{2+}$ stores and downregulation of capacitative $Ca^{2+}$ influx in Bcl-2–overexpressing cells. *J. Cell Biol.* 148:857–862.

Preston, G.A., J.C. Barrett, J.A. Biermann, and E. Murphy. 1997. Effects of alterations in calcium homeostasis on apoptosis during neoplastic progression. *Cancer Res.* 57:537–542.

Rizzuto, R., M. Brini, C. Bastianutto, R. Marsault, and T. Pozzan. 1995. Photoprotein-mediated measurement of calcium ion concentration in mitochondria of living cells. *Methods Enzymol.* 260:417–428.

Rizzuto, R., P. Pinton, W. Carrington, F.S. Fay, K.E. Fogarty, L.M. Lifshitz, R.A. Tuft, and T. Pozzan. 1998. Close contacts with the endoplasmic reticulum as determinants of mitochondrial $Ca^{2+}$ responses. *Science.* 280:1763–1766.

Roderick, H.L., J.D. Lechleiter, and P. Camacho. 2000. Cytosolic phosphorylation of calnexin controls intracellular $Ca^{2+}$ oscillations via an interaction with SERCA2b. *J. Cell Biol.* 149:1235–1248.

Sakuntabhai, A., V. Ruiz-Perez, S. Carter, N. Jacobsen, S. Burge, S. Monk, M. Smith, C.S. Munro, M. O'Donovan, N. Craddock, et al. 1999. Mutations in ATP2A2, encoding a $Ca^{2+}$ pump, cause Darier disease. *Nat. Genet.* 21:271–277.

Skryma, R., P. Mariot, X.L. Bourhis, F.V. Coppenolle, Y. Shuba, F.V. Abeele, G. Legrand, S. Humez, B. Boilly, and N. Prevarskaya. 2000. Store depletion and store-operated $Ca^{2+}$ current in human prostate cancer LNCaP cells: involvement in apoptosis. *J. Physiol.* 527:71–83.

Soulié, S., J.V. Moller, P. Falson, and M. le Maire. 1996. Urea reduces the aggregation of membrane proteins on SDS-PAGE. *Anal. Biochem.* 236:363–364.

Toyoshima, C., M. Nakasako, H. Nomura, and H. Ogawa. 2000. Crystal struc-

ture of the calcium pump of sarcoplasmic reticulum at 2.6 A resolution. *Nature.* 405:647–655.

Wertz, I.E., and V.M. Dixit. 2000. Characterization of calcium release-activated apoptosis of LNCaP prostate cancer cells. *J. Biol. Chem.* 275:11470–11477.

Wu, K.D., W.S. Lee, J. Wey, D. Bungard, and J. Lytton. 1995. Localization and quantification of endoplasmic reticulum $Ca^{2+}$-ATPase isoform transcripts. *Am. J. Physiol.* 269:C775–C784.

Wuytack, F., L. Raeymaekers, H. De Smedt, J.A. Eggermont, L. Missiaen, L. Van Den Bosch, S. De Jaegere, H. Verboomen, L. Plessers, and R. Casteels. 1992. $Ca^{2+}$-transport ATPases and their regulation in muscle and brain. *Ann. NY Acad. Sci.* 671:82–91.

Zhang, Y., J. Fujii, M. Phillips, H.-S. Chen, G. Karpati, W.-C. Yee, B. Schrank, D. Cornblath, K. Bobylan, and D. MacLennan. 1995. Characterization of cDNA and genomic DNA encoding SERCA1, the $Ca^{2+}$-ATPase of human fast-twitch skeletal muscle sarcoplasmic reticulum, and its elimination as a candidate gene for Brody disease. *Genomics.* 30:415–424.

Zhang, Z., D. Lewis, C. Strock, G. Inesi, M. Nakasato, H. Nomura, and C. Toyoshima. 2000. Detailed characterization of the cooperative mechanism of $Ca^{2+}$ binding and catalytic activation in the $Ca^{2+}$ transport (SERCA) ATPase. *Biochemistry.* 39:8758–8767.

Zhou, Y.P., D. Teng, F. Dralyuk, D. Ostrega, M.W. Roe, L. Philipson, and K.S. Polonsky. 1998. Apoptosis in insulin-secreting cells. Evidence for the role of intracellular $Ca^{2+}$ stores and arachidonic acid metabolism. *J. Clin. Invest.* 101:1623–1632.

Zhu, W.H., and T.T. Loh. 1995. Roles of calcium in the regulation of apoptosis in HL-60 promyelocytic leukemia cells. *Life Sci.* 57:2091–2099.